

Experimental determination of superconducting parameters for the intermetallic perovskite superconductor MgCNi_3

Z. Q. Mao, M. M. Rosario, K.D. Nelson, K. Wu*, I. G. Deac**, P. Schiffer, and Y. Liu[†]

Department of Physics, The Pennsylvania State University, University Park, PA 16802

T. He, K. A. Regan, and R. J. Cava

Department of Chemistry and Princeton Materials Institute, Princeton University, Princeton, NJ

08540

(October 28, 2018)

Abstract

We have measured upper-critical-field H_{c2} , specific heat C , and tunneling spectra of the intermetallic perovskite superconductor MgCNi_3 with a superconducting transition temperature $T_c \approx 7.6$ K. Based on these measurements and relevant theoretical relations, we have evaluated various superconducting parameters for this material, including the thermodynamic critical field $H_c(0)$, coherence length $\xi(0)$, penetration depth $\lambda(0)$, lower-critical-field $H_{c1}(0)$, and Ginsberg-Landau parameter $\kappa(0)$. From the specific heat, we obtain the Debye temperature $\theta_D \approx 280$ K. We find a jump of $\Delta C/\gamma T_c = 2.3$ at T_c (where γ is the normal state electronic specific coefficient), which is much larger than the weak coupling BCS value of 1.43. Our tunneling measurements revealed a gap feature in the tunneling spectra at Δ with $2\Delta/k_B T_c \approx 4.6$, again larger than the weak-coupling value of 3.53. Both findings indicate that MgCNi_3 is a strong-coupling superconductor. In addition, we observed a pronounced zero-bias conductance peak (ZBCP) in the tunneling spectra. We discuss the

possible physical origins of the observed ZBCP, especially in the context of the pairing symmetry of the material.

74.70.Dd, 74.25.Dw, 74.25.Bt, 74.50.+r

I. INTRODUCTION

Following the remarkable discovery of superconductivity at 39 K in MgB_2 ¹, intermetallic compounds have received renewed interest in the search for new superconducting materials. A new intermetallic superconductor, MgCNi_3 , with the superconducting transition temperature $T_c \approx 7.6$ K was found recently by He *et al.*². This compound has a cubic perovskite crystal structure, with Ni, C, and Mg replacing O, Ti and Sr, for example, in the more familiar oxide perovskite SrTiO_3 . It is a unique material that bridges the intermetallic compound MgB_2 and perovskite oxide superconductors.

The electronic structure of MgCNi_3 , calculated by several groups with different methods³⁻⁷, indicated that the electronic states of MgCNi_3 at the Fermi energy (E_F) are dominated by the $3d$ orbitals of Ni. The derived density of states (DOS) has a sharp peak just below E_F , which leads to a moderate Stoner enhancement. This signals the presence of substantial ferromagnetic (FM) spin fluctuations in MgCNi_3 ^{6,7}, as confirmed by ¹³C NMR measurements⁸. The presence of such FM fluctuations may favor unconventional pairing as in Sr_2RuO_4 ^{7,9}. However, the nuclear spin-lattice relaxation rate $1/T_1$ obtained in NMR measurements⁸ exhibited a clear coherence peak just below T_c , typical for an isotropic s -wave superconductor.

We measured the temperature dependence of resistivity in various magnetic field, and obtained the upper-critical field $H_{c2}(T)$ for this material. We also carried out the specific-heat measurements over a wider temperature region of 20-0.3 K on a high-quality MgCNi_3 sample. The value of T_c for this sample is 7.63 K as opposed to 6.2 K for the sample used in the previous measurements². From these measurements, we estimated various superconducting parameters of MgCNi_3 , including the thermodynamic critical field $H_c(0)$, coherence length $\xi(0)$, penetration depth $\lambda(0)$, lower-critical-field $H_{c1}(0)$, and Ginzberg-Landau (GL) parameter $\kappa(0)$.

The superconducting energy gap (Δ) of MgCNi_3 has been estimated from NMR measurements⁸, yielding a value of $2\Delta/k_B T_c \approx 3.2$ where T_c is the superconducting tran-

sition temperature. This value is less than the weak-coupling value of 3.53. However, our specific heat measurements revealed a jump of $\Delta C/\gamma T_c = 2.3$ (1.9 in Ref. 2) at the T_c of 7.63 K, considerably larger than the weak-coupling value 1.43, which is inconsistent with the NMR result.

To determine the superconducting gap directly, as well as to obtain information on the pairing symmetry of this new superconductor with apparently large ferromagnetic fluctuation similar to Sr_2RuO_4 , we have carried out tunneling spectroscopy measurements on high-quality polycrystalline MgCNi_3 samples. From these measurements, we found a gap feature with the ratio of $2\Delta/k_B T_c \approx 4.6$. This result, together with the specific heat data, suggests that MgCNi_3 is a strong-coupling superconductor. In addition, we observed a pronounced zero-bias conductance peak (ZBCP) in tunneling spectra. We discuss its possible physical origins, especially in the context of the pairing symmetry of the material.

II. EXPERIMENTAL

The polycrystalline material used for this study was synthesized by solid-state reaction. The preparation details can be found in Ref. [2]. We determined $H_{c2}(T)$ from four-probe resistance measurements. Specific heat measurements were performed using a relaxation method in a commercial calorimeter in a Quantum Design Physical Property Measurement System.

We prepared mechanical junctions for tunneling spectrum measurements. They were made on polycrystalline samples using a sharp W tip with an end radius of about 15 μm . The sample and the W tip were held together by an insulated Cu frame, with the tip touching the sample gently. The sample surface was examined by scanning electron microscopy. The average grain size on the surface was found to be about 5 μm . As a result, the mechanical tunnel junction involved only a few MgCNi_3 grains.

Current-voltage ($I-V$) characteristics, as well as junction resistance, was measured by a four-point method in a 1 K pot dip probe and a ^3He cryostat. To reduce heating, the $I-V$

curves were measured by a dc pulsed-current method with a typical pulse duration of 50 ms followed by a 2 s delay between successive pulses. The tunneling conductance ($G = dI/dV$) was computed numerically from the measured $I - V$ curves.

III. RESULTS AND DISCUSSIONS

A. Electrical transport

Figure 1 shows the $H - T$ phase diagram obtained from the R vs. T curves at different fields. Here T_c is defined as the intersection of the linear extrapolation of the most rapidly changing part of $R(T)$ and that of the normal state resistance, as shown in the inset of Fig. 1. Within the weak-coupling BCS theory, $H_{c2}(T = 0)$ can be estimated using the Werthamer-Helfand-Hohenberg (WHH) formula¹⁰,

$$\mu_0 H_{c2}(0) = -0.693(dH_{c2}/dT)_{T=T_c} T_c \quad (1)$$

which leads to a $\mu_0 H_{c2}(0)$ value of 14.8 T. Meanwhile the Pauli-limiting field

$$\mu_0 H^{\text{Pauli}} = 1.24 k_B T_c / \mu_B \quad (2)$$

expected within the same weak-coupling BCS theory¹¹ is about 14 T for $T_c = 7.60$ K. The $\mu_0 H^{\text{Pauli}}$ is about 0.8 T less than the $\mu_0 H_{c2}(0)^{\text{WHH}}$, suggesting that pair-breaking effects due to the Zeeman energy in MgCNi₃ is small. From our experimental results of specific heat and tunneling spectra, to be presented below, MgCNi₃ appears to be a strong-coupling superconductor. Taking into account the effects of strong coupling, a reasonable extrapolation of $H_{c2}(0)$ should lie between $\mu_0 H^{\text{Pauli}}$ and $H_{c2}(0)^{\text{WHH}}$, around 14.4 T, based on which the superconducting coherence length $\xi(0)$ can be estimated to be approximately 46 Å, using the GL formula for an isotropic three-dimensional superconductor, $\mu_0 H_{c2}(0) = \phi_0 / 2\pi \xi(0)^2$. This value is in good agreement with a earlier report of $\xi(0) = 47$ Å.¹²

B. Specific heat

We measured the specific heat of MgCNi₃ from 20 K down to 0.4 K. As shown in the inset of Fig. 2, the specific-heat data in the temperature region of $T_c^{onset}(\approx 9.4 \text{ K}) < T < 16 \text{ K}$, was fitted well with the form $C(T) = \gamma T + \beta T^3$, which is the usual temperature dependence of specific heat for metals at $T \ll \Theta_D$. The Θ_D can be determined from the coefficient of the T^3 term $\beta = N(12/5)\pi^4 R \Theta_D^{-3}$, where $R=8.314 \text{ J/mol-K}$, and $N=5$ for MgCNi₃. The linear term of $C(T)$ is due to the electronic contribution, while the T^3 term comes from the phonon contribution. From the above fitting, we obtained $\gamma=9.2 \text{ mJ/mol-Ni.K}^2$ and $\Theta_D \approx 280 \text{ K}$.

By subtracting the phonon contribution from the $C(T)$, we obtained the temperature dependence of electronic specific heat $C_e(T)$. The main panel of Fig. 2 shows C_e/T as a function of T . It reveals a much sharper superconducting transition than seen in the specific-heat data in Ref. 2. From an entropy-conserving construction (see the solid lines in the figure), the midpoint transition temperature T_c^{mid} was estimated to be 7.63 K, and the specific-heat jump $\Delta C/T_c^{mid} = 21.1 \text{ mJ/mol-Ni K}^2$. This value is considerably larger than that reported in Ref. 2 where $\Delta C/T_c^{mid} = 19.0 \text{ mJ/mol-Ni.K}^2$ with $T_c^{mid} = 6.2 \text{ K}$, indicating that the sample used in the present study is of improved quality. On the other hand, we note that the C_e/T shows an unusual behavior at low temperature, i.e., an upturn for $T < 2 \text{ K}$. This upturn is most likely due to the paramagnetism of unreacted Ni impurities. Similar behavior was observed in MgB₂ where Fe impurities led an upturn in C/T at low temperature¹³.

It is known that the parameter $\Delta C(T_c)/\gamma T_c$ can be used to measure the strength of the electron coupling¹⁴. In the BCS weak-coupling limit, its value is 1.43. For MgCNi₃, the ratio of $\Delta C(T_c)/\gamma T_c$ estimated from the above data is approximately 2.3 (1.9 in Ref. 2), much larger than the weak coupling value. This indicates that MgCNi₃ is a strong-coupling superconductor with coupling strength close to that of Hg with $\Delta C(T_c)/\gamma T_c = 2.37$. This is consistent with our results of tunneling measurements (see below).

Based on the specific data and $H_{c2}(0)$ obtained above, we can estimate various superconducting parameters using relevant theoretical relations for isotropic 3D superconductor. The $H_c(0)$ can directly be estimated by integrating the specific data of Fig. 2 in the superconducting state and using the relation:

$$\mu_0 H_c(0)^2/2 = -\gamma T_c^2/2 + \int_0^{T_c} C_e(T) dT. \quad (3)$$

The $\mu_0 H_c(0)$ thus evaluated is 0.22 T. The GL parameter κ was evaluated from

$$H_{c2}(0) = \sqrt{2}\kappa H_c(0) \quad (4)$$

to be 46, which is quite large, but not as large as that of high- T_c superconductors¹⁵. From $\kappa = \lambda/\xi$, the estimated penetration depth is $\lambda(0) = 2130 \text{ \AA}$. Using

$$H_{c1}(0)H_{c2}(0) = H_c(0)^2(\ln\kappa(0) + 0.08) \quad (5)$$

valid for $\kappa \gg 1$, the lower critical field H_{c1} was estimated to be 13 mT. All estimated parameters are summarized in Table 1.

C. Single-particle tunneling

Figure 3 displays a set of typical tunneling conductance spectra (G vs. V) of MgCNi₃ (Junction MCN/W #6). The junction resistance, $R_J(T)$, measured at 0.4 mA (corresponding to a voltage below 0.02 mV for $T < 8$ K), started to drop at the bulk T_c , 7.63 K, as shown in the left inset where bulk resistivity is also included for comparison. This drop was much broader than the transition seen in bulk resistivity, suggesting that the junction resistance must have been dominated by the tunnel barrier. Therefore the voltage drop should primarily occur at the junction interface.

As seen in the main panel of Fig. 3, the dominant feature, a pronounced zero-bias conductance peak (ZBCP) accompanied by two dips, starts to develop around the bulk T_c . The dip feature had a smooth, clearly identifiable temperature dependence up to bulk T_c . Therefore, the energy where G shows a sharp drop (as indicated by arrows in Fig.

3), is clearly a characteristic energy E_c associated with the bulk phase of MgCNi₃. If we identify this energy as the superconducting gap Δ , we estimated the $\Delta(0)$ for MgCNi₃ to be 1.5 meV, with $2\Delta/k_B T_c \approx 4.6$. This ratio is larger than the BCS weak-coupling value, 3.53, but close to that of strong coupling superconductor Hg ($2\Delta/k_B T_c \approx 4.3$), consistent with the indication obtained from the specific-heat measurement. The right inset of Fig. 3 shows the temperature dependence of E_c for this junction. For comparison, we include the $\Delta(T)$ in the weak-coupling BCS model into this inset (dashed line). Clearly the $E_c(T)$ obtained as described above is higher than the $\Delta(T)$ of weak-coupling BCS at lower temperatures, again supporting the statement that MgCNi₃ is a strong-coupling superconductor.

Figure 4 shows the tunneling spectra of another junction (MCN/W #4) measured down to 0.4 K. The tunneling features seen in this junction look somewhat different from junction MCN/W #6 shown in Fig.3: the conductance peak was much broader and did not split at higher temperatures (> 3 K); but evolved into a spectrum of sharper central ZBCP with two side peaks as $T < 3$ K. We believe that such a difference is most likely caused by distinct barrier strength at the junction interface. Nevertheless, the characteristic energy E_c defined using the same way as described above (see the arrows in Fig.4) seems comparable to that defined in junction MCN/W #6.

It is interesting to consider the possible physical origins of the ZBCPs observed in the tunneling spectra. First, it is known that magnetic impurities in or near the barrier can lead to a ZBCP due to magnetic and Kondo scattering (the Appelbaum-Anderson model)¹⁶. For the MgCNi₃ samples used in the present study, a small amount of unreacted Ni was very likely to exist, as reflected in the specific-heat measurement. It might appear near the tunnel barrier as a magnetic impurity. However, a ZBCP due to magnetic impurities should be uncorrelated with the occurrence of superconductivity. In contrast, the ZBCP in the present case was found to emerge just below bulk T_c . In addition, the height of the ZBCP caused by magnetic impurities should depend on temperature logarithmically¹⁶, which was not found in our experiment. Further, in the Appelbaum-Anderson model, a magnetic field should split the ZBCP. But in our experiment, we found that the ZBCP became sharper

under a magnetic field, instead of splitting, as shown in the right inset of Fig. 4. Therefore, magnetic impurities cannot be responsible for the observed ZBCP in MgCNi₃.

Although our tunnelling spectra were obtained at a superconductor/normal-metal (S/N) interface, the observed ZBCP cannot be due to conventional Andreev reflection. The values of $G_s/G_n(V = 0)$ (G_n is the normal state zero-bias conductance at 8 K), which were found to be around 5 in these two junctions discussed above, were considerably larger than the maximum value of 2 expected for the conventional Andreev reflection¹⁷.

Another mechanism for the ZBCP that is particularly relevant to our experiment is related to Josephson-coupling effects. The junctions we used for this study were prepared on polycrystalline samples. These samples could consist multiple junctions formed between W tip and MgCNi₃ grains. Each of these grains was in turn connected with other MgCNi₃ grains, forming parallel conduction channels. Each channel would then consist a W/MCN junction and additional MCN/MCN junctions in series. The Josephson coupling at a dominating intergrain interface may result in a large ZBCP in the tunneling spectrum, as observed in tunnel junctions prepared on polycrystalline MgB₂¹⁸. However, the ZBCP originating from intergrain interface should grow rapidly in height with decreasing temperature because of the emergence of Josephson coupling at low temperatures. Our observation of the saturation in the height of $dI/dV(V = 0)$ below 2.0 K (see the left inset of Fig.4) is not consistent with such a simple intergrain-coupling picture. To completely rule out the intergrain coupling as the origin of the observed ZBCP, more experiments on single crystal samples, which have not been available yet, are certainly necessary.

Can the observed ZBCP be due to the surface mid-gap Andreev Bound states (ABSs)^{19,20} of a non-*s*-wave superconductor? ABSs arise from quantum interference during the Andreev reflection at the surface of an unconventional superconductor where the scattered quasi-particles experience a phase change. ABSs manifest as a ZBCP, as observed in *d*- and *p*-wave superconductors²¹⁻²⁴. To examine if there is such a possibility for our ZBCP observations, we have estimated the temperature dependence of spectral weight of central ZBCP and side peak in Fig. 4 by integrating G/G_n in the appropriate ranges of V . It was found that a clear

spectral-weight transfer from the side peak to the ZBCP occurs with decreasing temperature. This suggests that the ABSs is a possible origin for the ZBCP observed in MgCNi₃. Therefore we should not exclude the possibility of unconventional pairing in MgCNi₃. Our suggestion seems consistent with a recent result of band calculations that indicates that MgCNi₃ is near a ferromagnetic instability and its superconductivity is unconventional in nature⁷.

However, as pointed earlier, NMR measurements revealed a coherence peak in $1/T_1$ just below T_c ⁸, which appears to suggest that MgCNi₃ is an *s*-wave superconductor. This seems to contradict to our observation and the theoretical indication⁷. More experiments are clearly needed to reconcile the apparently opposite indications offered by these two types of measurements. If the pairing symmetry in MgCNi₃ turns out to be indeed *s*-wave, then our observation of the anomalous behavior in the ZBCP will still be of interest as it demands a new model for the ZBCP within the framework of *s*-wave superconductivity.

Finally, we comment on why the coupling strength estimated from NMR⁸ is inconsistent with that reflected in specific-heat and tunneling measurements. The ratio of $2\Delta/k_B T_c (=3.2)$ evaluated by NMR was obtained from the exponential fit of the temperature dependence of $1/T_1$ (measured at 0.45 T). In principle, the most reliable Δ value should be obtained by the fit of $1/T_1$ to temperatures much lower than T_c to avoid the crossover regime. However, the $1/T_1$ fit in Ref. [8] was extended only down to 2.5 K. Below this temperature, the $1/T_1$ became saturated. This saturation behavior was ascribed to the flux avalanche effect. If the diminished temperature range resulted in a low estimate of Δ , then these NMR data and the present specific-heat and tunneling results might be reconciled.

IV. CONCLUSION

In conclusion, we have carried out upper-critical field, specific heat and tunneling spectroscopy measurements of the newly discovered intermetallic perovskite superconductor MgCNi₃. We have evaluated various superconducting parameters using the specific heat data and $H_{c2}(0)$. The specific heat measurement gives $\Delta C/\gamma T_c = 2.3$ and the Debye tem-

perature, $\theta_D \approx 280$ K, indicating that MgCNi_3 is a strong-coupling superconductor. We have also seen a corresponding signature of strong coupling in the tunneling measurement of MgCNi_3 , which reveals a gap feature with the ratio of $2\Delta/k_B T_c \approx 4.6$. In addition, from the presence of a ZBCP in tunneling spectra of MgCNi_3 , we suggest that the possibility of unconventional pairing in MgCNi_3 should not be excluded even though the NMR experiment suggests that it is a *s*-wave superconductor. Additional experimental probes, as well as single crystal samples, are needed to further elucidate the pairing symmetry of this novel superconductor.

We would like to thank T. Imai, D.J. Singh, I.I. Mazin and N-C. Yeh for useful discussions. This work was supported at Penn State by NSF through Grants No. DMR-9974327, DMR-0101318 and DMR-9702661, and at Princeton by NSF grants DMR-9809483 and DMR-9725979, and DOE through grant DE-FG02-98-ER45706.

REFERENCES

- * Permanent address: Department of Physics, Peking University, Beijing, PRC
- ** Permanent address: Department of Physics, Babes-Bolyai University, Cluj-Napoca, Romania
- † E-mail: liu@phys.psu.edu
- ¹ J. Nagamatsu, N. Nakagawa, T. Muranaka, Y. Zenitani, J. Akimitsu, *Nature* **410**, 63 (2001).
- ² T. He, Q. Huang, A.P. Ramirez, Y. Wang, K.A. Regan, N. Rogado, M. A. Hayward, M. K. Haas, J.S. Slusky, K. Inumara, H.W. Zandbergen, N.P. Ong, R.J. Cava, *Nature* **411**, 54 (2001).
- ³ A. Szajek, *J. Phys.: Condens Matter*, **13**, L595 (2001).
- ⁴ S.B. Dugdale and T. Jarlborg, *Phy. Rev. B* **64**, R100508 (2001).
- ⁵ J.H. Shim and B.I. Min, *Phy. Rev. B* **64**, R180510 (2001).
- ⁶ D.J. Singh and I.I. Mazin, *Phy. Rev. B* **64**, R140507 (2001).
- ⁷ H. Rosner, R. Weht, M. D. Johannes, W. E. Pickett, and E. Tosatti, *Phy. Rev. Lett.* **88**, 027001 (2002).
- ⁸ P. M. Singer, T. Imai, T. He, M. A. Hayward, and R. J. Cava, *Phy. Rev. Lett.* **87**, 257601 (2001).
- ⁹ Y. Maeno, T. M. Rice, and M. Sigrist, *Phys. Tod.* **54**, 42 (2001).
- ¹⁰ N. R. Werthamer, E. Helfand, and P. C. Hohenberg, *Phys. Rev.* **147**, 295 (1966).
- ¹¹ A. M. Clogston, *Phys. Rev. Lett.* **9**, 266 (1962).
- ¹² S. Y. Li, R. Fan, X. H. Chen, C. H. Wang, W. Q. Mo, K. Q. Ruan, Y. M. Xiong, X. G. Luo, H. T. Zhang, L. Li, Z. Sun, and L. Z. Cao, *Phys. Rev. B* **64**, 132505 (2001).

- ¹³ Y. Wang, T. Plackowski, and A. Junod, *Physica C* **355**, 179 (2001).
- ¹⁴ H. Padamasee, J. E. Neighbor, and C.A. Shiffman, *J. Low. Temp. Phys.* **12**, 387 (1973).
- ¹⁵ A. Junod, in: A. Narlikar (Ed.), *Studies of High Temperature Superconductors*, Vol. 19, Nova Science Publishers, Commack, Ny, 1996.
- ¹⁶ J. Appelbaum, *Phys. Rev. Lett.* **14**, 91 (1966).
- ¹⁷ G. E. Blonder, M. Tinkham, and T. M. Klapwijk, *Phys. Rev. B* **25**, 4515 (1982).
- ¹⁸ H. Schmidt, J. F. Zasadzinski, K. E. Gray, and D. G. Hinks, *Phys. Rev. B* **63**, R220504 (2001).
- ¹⁹ C. R. Hu, *Phys. Rev. Lett.* **72**, 1526 (1994).
- ²⁰ Y. Tanaka and S. Kashiwaya, *Phys. Rev. Lett.* **74**, 3451 (1995).
- ²¹ L. H. Greene, M. Covington, M. Aprili, E. Badica, D. E. Pugel, *Physica B* **280**, 159 (2000).
- ²² J. Y. T. Wei, N.-C. Yeh, D. F. Garrigus, and M. Strasik, *Phys. Rev. Lett.* **81**, 2542 (1998).
- ²³ F. Laube, G. Goll, H. v. Lhneysen, M. Fogelstrm, and F. Lichtenberg, *Phys. Rev. Lett.* **84**, 1595 (2000).
- ²⁴ Z. Q. Mao, K. D. Nelson, R. Jin, Y. Liu, and Y. Maeno, *Phys. Rev. Lett.* **87**, 037003 (2001).

FIGURES

FIG. 1. Upper critical field $\mu_0 H_{c2}$ as a function of temperature for MgCNi₃. The square symbol is $\mu_0 H_{c2}(0)$ estimated using WHH theory and the triangle is the estimated Pauli-limiting field (see text). The inset shows the temperature dependence of sample resistance in zero field.

FIG. 2. Temperature dependence of the electronic specific heat divided by temperature, C_e/T , of MgCNi₃. The inset shows the C/T as a function of T^2 above T_c . The solid line is the fit of the experimental data to $C = \gamma T + \beta T^3$ between 9.5 and 16 K.

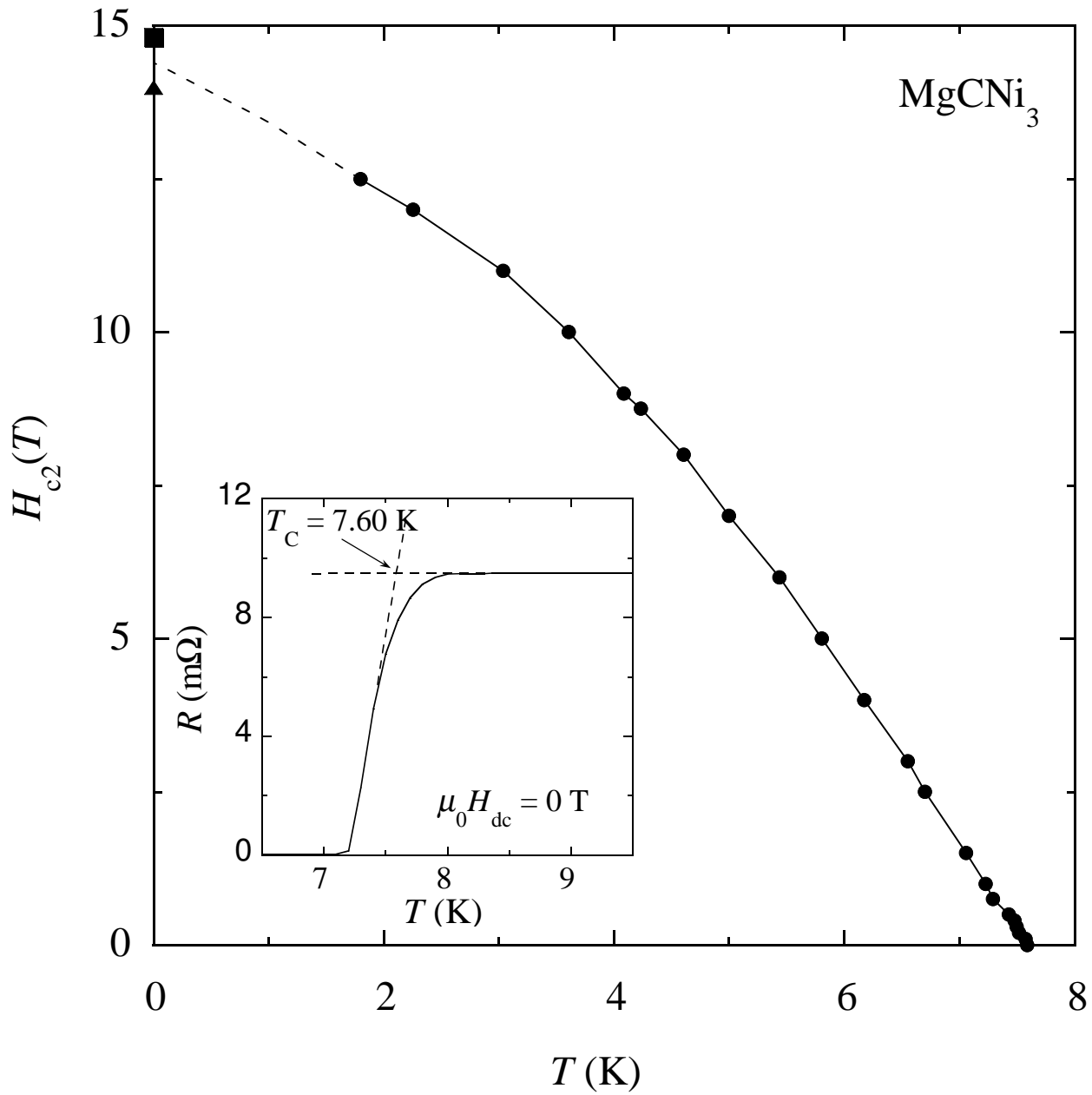
FIG. 3. Tunneling spectra of $G=dI/dV \sim V$ (on a logarithmic scale) for junction MCN/W #6 at different temperatures. All curves except the top curve have been shifted downwards for clarity by multiplying G with a numerical factor. The left inset shows the junction resistance $R_J(T)$ and bulk resistivity. The right inset shows the temperature dependence of the characteristic energy E_c , as well as the BCS $\Delta(T)$.

FIG. 4. Tunneling conductance spectra (on a logarithmic scale) for junction MCN/W #4. All curves except the top curve have been shifted downwards for clarity by multiplying G with a numerical factor. The left inset shows the $R_J(T)$ of junction MCN/W #4, measured at 1mA (corresponding to a voltage below 0.08 meV for $T < 8$ K). The right inset shows tunneling conductance spectra of junction MCN/W #4 measured under fields of 0 T and 0.5 T at 1.5 K.

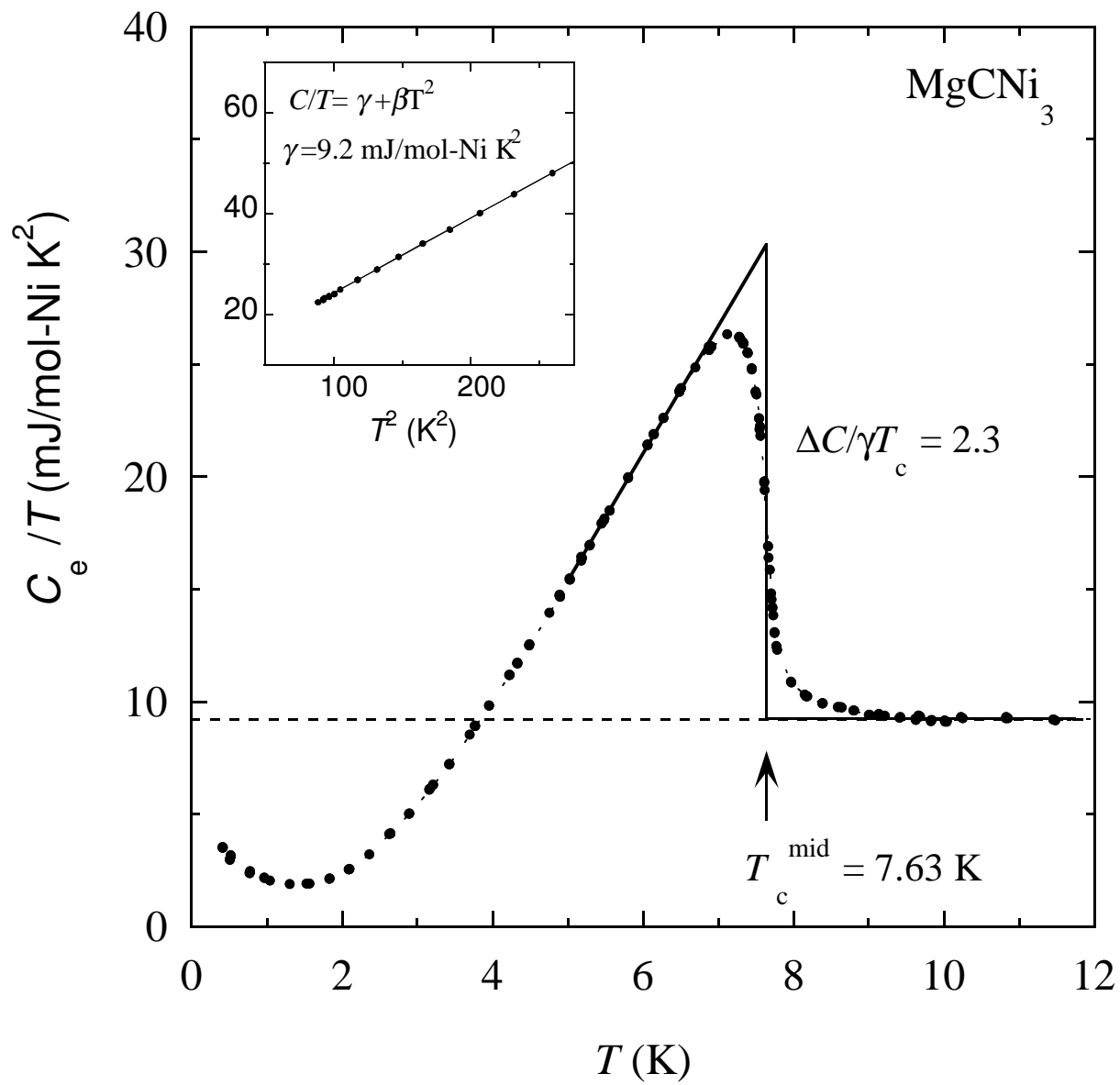
TABLES

TABLE I. Characteristic parameters of intermetallic perovskite superconductor MgCNi₃

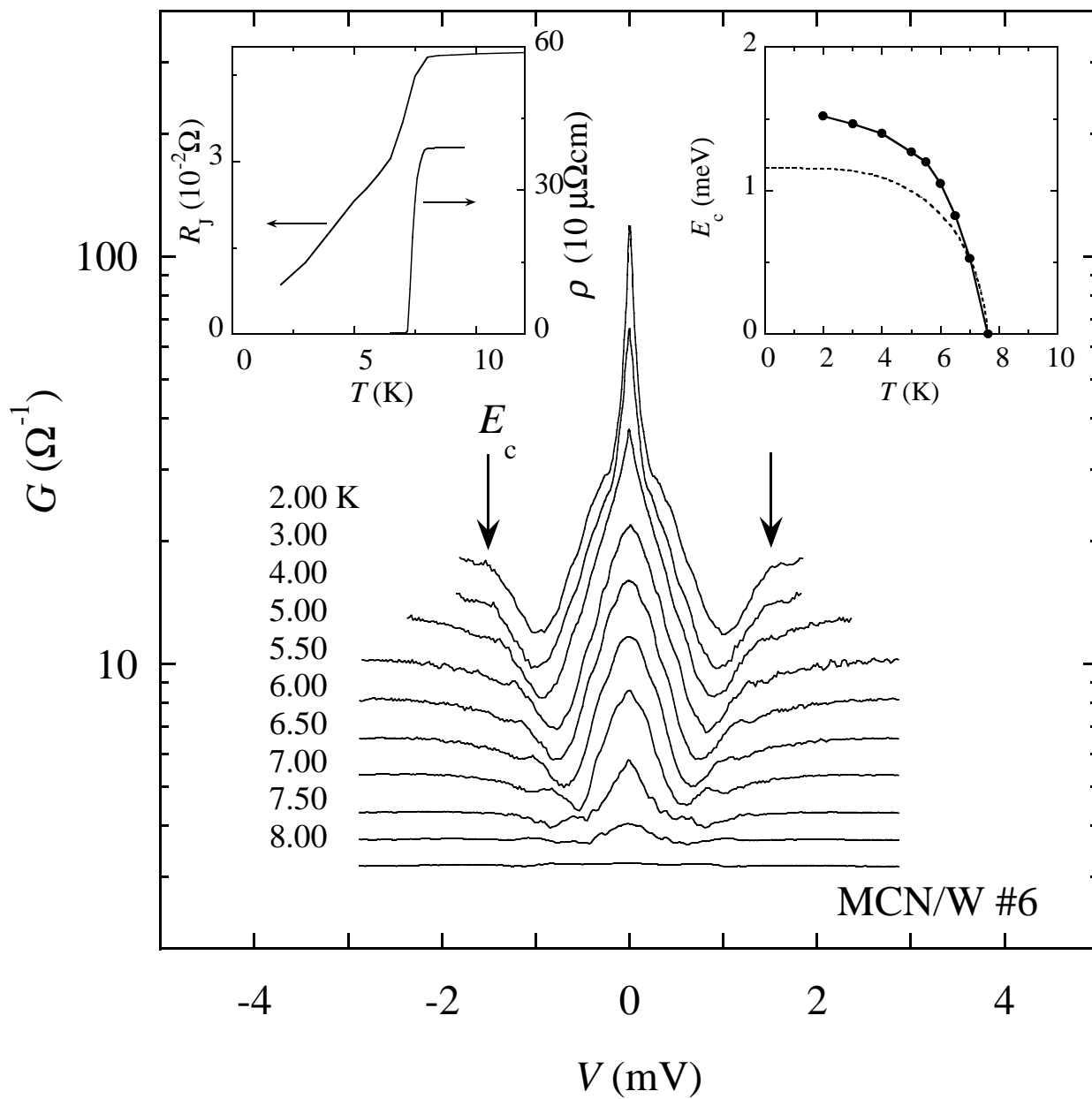
| Parameters |
|---|
| $T_c = 7.63$ K |
| $\mu_0 H_{c2}(0) = 14.4$ T |
| $\mu_0 H_c(0) = 0.22$ T |
| $\mu_0 H_{c1}(0) = 13$ mT |
| $\xi(0) = 46$ Å |
| $\lambda(0) = 2130$ Å |
| $\kappa(0) = 46$ |
| $\gamma = 9.2$ mJ/mol-Ni.K ² |
| $\Theta_D = 280$ K |
| $\Delta C/\gamma T_c = 2.3$ |
| $2\Delta/k_B T_c = 4.6$ |



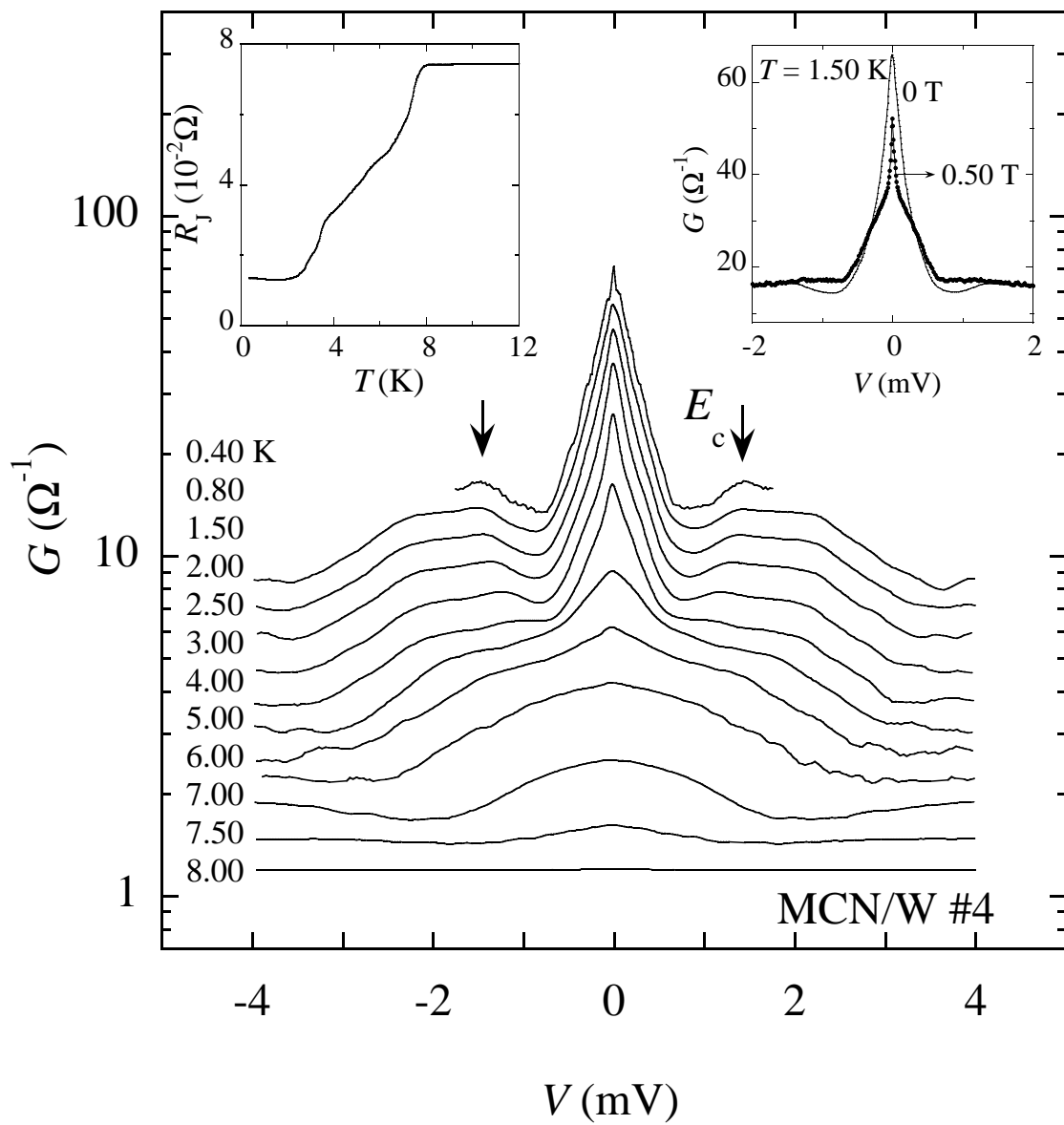
Mao *et al.*, Figure 1



Mao *et al.*, Figure 2



Mao *et al.*, Figure 3



Mao *et al.*, Figure 4